Altered structural brain networks in refractory and non-refractory idiopathic generalised epilepsy

Andrea McKavanagh[1,2], Barbara A.K. Kreilkamp[1,2,3], Yachin Chen[1,2], Christine Denby[2], Martyn Bracewell[2,4], Kumar Das[2], Christophe De Bezenac[1,2], Anthony G. Marson[1,2], Peter N. Taylor[5], Simon S. Keller[1,2]*

[1]Department of Pharmacology and Therapeutics, Institute of Systems, Molecular and Integrative Biology, University of Liverpool, UK
[2] Department of Neuroradiology, The Walton Centre NHS Foundation Trust, Liverpool, UK
[3] Department of Neurology, University Medicine Göttingen, Göttingen, Germany
[4]Schools of Medical Sciences and Psychology, Bangor University, Bangor, UK
[5]Interdisciplinary Computing and Complex BioSystems Group, School of Computing Science and Institute of Neuroscience, Faculty of Medical Science, Newcastle University, UK

*Corresponding author:

Dr Simon S. Keller

Clinical Sciences Centre, Aintree University Hospital, Lower Lane, Liverpool, L9 7LJ.

Simon.Keller@liverpool.ac.uk

Running header: Structural Networks and IGE

Keywords: Connectome, Genetic Generalised Epilepsy, Epilepsy, MRI, biomarker, outcome

Abstract

Background: Idiopathic generalised epilepsy (IGE) is a collection of generalised non-lesional epileptic network disorders. Around 20−40% of patients with IGE are refractory to anti-seizure medication and mechanisms underlying refractoriness are poorly understood. Here, we characterise structural brain network alterations and determine whether network alterations differ between patients with refractory and non-refractory IGE.

Methods: Thirty-three patients with IGE (10 non-refractory and 23 refractory) and 39 age and sex-matched healthy controls were studied. Network nodes were segmented from T1-weighted images while connections between these nodes (edges) were reconstructed from diffusion MRI. Diffusion networks of fractional anisotropy (FA), mean diffusivity (MD), radial diffusivity (RD) and streamline count (Count) were studied. Differences between all patients, refractory, non-refractory and control groups were computed using Network Based Statistics. Nodal volume differences between groups were computed using Cohen's d effect size calculation.

Results: Patients had significantly decreased bihemispheric FA and Count networks and increased MD and RD networks compared to controls. Alterations in network architecture, with respect to controls, differed depending on treatment outcome, including predominant FA network alterations in refractory IGE and increased nodal volume in non-refractory IGE. Diffusion MRI networks were not influenced by nodal volume.

Discussion: Although a non-lesional disorder, patients with IGE have bihemispheric structural network alterations which may differ between patients with refractory and non-refractory IGE. Given that distinct nodal volume and FA network alterations were observed between treatment outcome groups, a multifaceted network analysis may be useful for identifying imaging biomarkers of refractory IGE.

Impact Statement

Although it is accepted that epilepsy is a network disorder, few studies have prospectively recruited patients with clear refractory and non-refractory idiopathic generalised epilepsy (IGE) with a goal to identify MRI markers of pharmacoresistance. By showing that patients with refractory and non-refractory IGE have different patterns of diffusion MRI networks and nodal volume alterations with respect to controls, we suggest that imaging analysis of structural networks may have the potential to identify unique biomarkers of treatment outcome. Reliable imaging markers of pharmacoresistance could inform the treatment pathway for many patients with epilepsy.

Introduction

Idiopathic Generalised Epilepsy (IGE), also referred to as genetic generalised epilepsy (Scheffer *et al.*, 2017), is a collection of presumably genetically based generalised epileptic disorders (Berg *et al.*, 2010; Scheffer *et al.*, 2017), which account for 15 − 20% of all epilepsies (Jallon and Latour, 2005). The disorder is characterised clinically by generalised seizures, spike and polyspike-wave discharges on EEG (Seneviratne, Cook and D'Souza, 2012) and no visible anatomical brain lesions on MRI. Despite available anti-seizure medication (ASM) treatment, 20−40% of patients with IGE are refractory to medication and continue to have debilitating seizures (Cockerell *et al.*, 1995; Semah *et al.*, 1998; Baykan *et al.*, 2008). The mechanisms underlying refractoriness after ASM remain unknown and currently there are no reliable biomarkers of treatment outcome.

Although, by definition, patients with IGE are non-lesional, advanced quantitative MRI techniques have identified volumetric and microstructural brain alterations in patients relative to healthy controls in group comparison studies. A meta-analysis of twelve voxel-based morphometry (VBM) IGE studies reported structural alterations showing grey matter atrophy in the thalamus and increased grey matter volume in the right medial frontal gyrus and

cingulate cortex in patients with IGE (Bin *et al.*, 2017). Reduced cortical thickness has also been reported in frontal lobe regions in patients with IGE (Bernhardt *et al.*, 2009). Using a graph theory approach on structural covariance networks, studies have found widespread altered topological organisation of grey matter (Liao *et al.*, 2013; Sone *et al.*, 2019). Diffusion tensor imaging (DTI) alterations in white matter tracts have also been reported. Reduced fractional anisotropy (FA) (Liu *et al.*, 2011; Vulliemoz *et al.*, 2011; Focke *et al.*, 2014; Lobato *et al.*, 2018) and increased mean diffusivity (MD) (Focke *et al.*, 2014; Lobato *et al.*, 2018) and radial diffusivity (RD) (Focke *et al.*, 2014) have been found in major white matter tract bundles. Affected tracts include the corpus callosum, superior and inferior longitudinal fasciculi and the uncinate fasciculi.

Epilepsy is a network disorder with aberrant alterations of interactions between brain regions, which can cause functional impairments leading to epileptic seizures (Spencer, 2002; Kramer and Cash, 2012; van Diessen *et al.*, 2013; Bernhardt, Bonilha and Gross, 2015). Brain networks can be reconstructed from DTI, a clinically feasible neuroimaging method that models water diffusion properties within brain tissue (Qi *et al.*, 2015). Increased streamline count connectivity has been found in the primary motor, parietal and subcortical regions in patients with IGE relative to controls (Caeyenberghs *et al.*, 2015). Furthermore, altered topological network properties have been found in DTI-based networks of patients with IGE using graph theoretical approaches (Zhang *et al.*, 2011; Xue *et al.*, 2014; Qiu *et al.*, 2017). These altered structural brain networks could provide new insights into functional impairments leading to epileptic seizures and could translate into potential biomarkers for treatment outcome in patients with IGE.

Despite an increasing number of published studies on brain networks in IGE, there are limited insights into potential network biomarkers of pharmacoresistence of the disorder. The aim of this study was to identify biomarkers of pharmacoresistant seizures in IGE by comparing structural network alterations in pharmacologically well-controlled (non-refractory)

and uncontrolled (refractory) patients with IGE relative to healthy controls using a network-based statistics (NBS) approach (Zalesky, Fornito and Bullmore, 2010). Given that many studies report singular diffusion network parameter alterations in IGE (O'Muircheartaigh *et al.*, 2012; Caeyenberghs *et al.*, 2015), we analysed diffusion network alterations with respect to streamline count (Count; the number of streamlines within a voxel), fractional anisotropy (FA; the measurement of anisotropic diffusion inferring directionality), mean diffusivity (MD; measuring the average magnitude of diffusion in all directions), axial diffusivity (AD; the magnitude of diffusion parallel to the principle direction of diffusion), and radial diffusivity (RD; the magnitude of diffusion radially to the principle direction of diffusion in every voxel). By analysing multiple diffusion measures we increase the probability of understanding disruptions to the microstructural environment in IGE. We supplemented our NBS diffusion network approach with volumetric analysis of cortical nodes to determine whether diffusion networks were related to morphometric alterations in cortical and subcortical grey matter structure.

Methods

Participants

We recruited 33 patients with a diagnosis of IGE (mean age 32 ± 15 years, 18 females, 15 males). All patients were recruited from the Walton Centre NHS Foundation Trust and informed written consent was obtained for all participants (local research ethical committee reference 14/NW/0332). All patients were diagnosed with IGE by a consultant neurologist based on the ILAE classification of seizure semiology (Fisher *et al.*, 2017), patient history and EEG findings (generalised spike/polyspike-wave changes). IGE sub-syndromes were classified as absence epilepsy (childhood or juvenile), juvenile myoclonic epilepsy or generalised epilepsy with tonic-clonic seizure on waking. There were no potentially epileptogenic or incidental brain lesions on diagnostic MRI. Twenty-three patients had refractory IGE despite ASM treatment and ten were non-refractory. Patients were recruited prospectively and classified as non-refractory if they had no seizure activity over a one year period prior to scanning (Kwan *et al.*, 2010). Patients that presented with two or more seizures one year prior to scanning were termed refractory (Kwan *et al.*, 2010). A comparison of demographic and clinical data between refractory and non-refractory patients is shown in Table 1. We additionally recruited 39 age and sex matched healthy controls (Table 1). Furthermore, detailed clinical characteristics of patients recruited with IGE including specific sub-syndromes and medication regimes are included in Table 2.

MRI acquisition

Participants were scanned at the Department of Neuroradiology at the Walton Centre NHS Foundation Trust on a 3T GE Discovery MR 750 MRI scanner with a 32-channel head coil. Structural 3D T1-weighted (T1w) and diffusion weighted (DW) images were acquired. The specifications were as follows: T1w fast-spin-gradient images with Phased Array Uniformity

Enhancement signal inhomogeneity correction (140 slices, TR=8.2 ms, TI=450 ms, TE=3.22 ms, flip angle=12, with 1mm isotropic voxel size, acquisition time: 3:48 mins). DW imaging included a 60 direction spin echo pulse sequence (66 slices, TR = 8000ms, TI = N/A, TE = 82 ms, flip angle = 90, voxel size = 1mm x 1mm x 2mm, no cardiac gating, with ASSET, b-value = 1000 s/mm2, FOV = 256 mm, with six b0 images without diffusion weighting, acquisition time: 8:56 minutes).

Image preprocessing

The T1w images were preprocessed using FreeSurfer's (v6.0) recon all function for cortical and subcortical reconstruction, which includes pre-processing (motion correction, image inhomogeneity correction, skull stripping), tissue specific segmentation, subcortical and cortical labelling, surface reconstruction and cortical parcellation (https://surfer.nmr.mgh.harvard.edu). The Desikan Killiany atlas (Desikan *et al.*, 2006) was used to parcellate images into 82 regions of interest across the entire brain. The parcellated regions underwent quality control inspection and were manually corrected if necessary.

DW images were corrected for artefacts using FMRIB's (Oxford Centre for Functional MRI of the Brain) FSL (v6.0) software (www.fmrib.ox.ac.uk/fsl, (Smith *et al.*, 2004) according to the diffusion MRI pre-processing steps of the ENIGMA pipeline (http://enigma.ini.usc.edu/protocols/dti-protocols/) which included TOPUP for echo-planar image distortion correction and EDDY for motion and eddy current correction. Image reconstruction and deterministic tractography of DTI was performed in DSI studio (Build 27-02-2019, http://dsi-studio.labsolver.org). The diffusion data were reconstructed using generalized q-sampling imaging (Yeh, Wedeen and Tseng, 2010) with a diffusion sampling length ratio of 1.25. We chose a deterministic fibre tracking algorithm (Yeh *et al.*, 2013) as there is an increased likelihood of false positives connections from probabilistic approaches (Sarwar *et al.*, 2019). The whole brain was used as a seed region. The quantitative anisotropy threshold was 0.1, the angular threshold was 60 degrees, and the step size was

1 mm. Streamlines with length shorter than 10 or longer than 300 mm were discarded and a total of 1000000 streamlines were calculated. Topology-informed pruning (Yeh *et al.*, 2019) was applied to the tractography with 1 iteration to reduce the number of false connections.

Structural networks

Structural connectivity networks were built from T1w and DW scans (Figure 1.A) in native space using DSI studio (Build 27-02-2019). A structural brain network can be mathematically described as a graph with nodes representing brain regions and edges forming connections between those regions. For our analysis, network nodes consisted of the 82 segmented T1w regions as used in previous connectivity analysis (Munsell *et al.*, 2015; Taylor *et al.*, 2015, 2018). Network edges consisted of connection weights between nodes which were reconstructed using the diffusion MRI data for Count, FA, MD, AD and RD. For two patients grey matter dilation of one node was performed to prevent the disconnection of that node caused by premature tracking termination (Wei *et al.*, 2017).

DSI studio outputs a weighted connectivity matrix representing the structural network. Connectivity matrices were constructed with matrix entries (C_{ij}) representing a connection between two nodes (*i* and *j*). Network edges were retained if one or more streamlines terminated between the two corresponding nodes. Connectivity matrices were thresholded to ensure matrix inputs contained connections present in at least 75% of all participants in all groups and were common to every group (Besson *et al.*, 2014). We used an absolute threshold method which applies a uniform threshold to keep connections above a fixed connection strength which has been found to be advantageous for removing spurious connections in structural networks (Buchanan *et al.*, 2019).

Statistical Network analysis

Network differences between patient and control groups were compared using NBS (Zalesky, Fornito and Bullmore, 2010) (Figure 1.B). Global unpaired NBS t-tests were performed between patient and control groups. Age and sex were added as covariates for all metrics and intracranial volume (ICV) obtained from FreeSurfer segmentation was added as an additional covariate for streamline count. NBS uses T-score thresholding to control for Type I errors. We therefore validated the stability of significant findings at multiple thresholds (range = 1.5 - 4.0, with increments of 0.1). NBS then clustered significantly different edges into networks and provided a family-wise error rate (FWER) corrected p-value for each network cluster using 10,000 permutations. For more details on the NBS method see Zalesky et al., (Zalesky, Fornito and Bullmore, 2010). Results are shown at an intermediate threshold of $|T|>2.7$. P values associated with this T score are $p=0.008$ (all patients and controls, n=72; refractory and controls, n=62) and $p=0.009$ (non-refractory and controls, n=49), which was considered a stringent statistical threshold.

Along with NBS, network differences between patients with refractory and non-refractory IGE were compared using Cohen's d effect size calculation due to the small sample size of the patient groups (n=33). Effect size small sample size correction (n<50) as previously described (Durlak, 2009) was also applied. Effect sizes can provide important information on whether legitimate differences exist between groups of participants despite the lack of significant differences using conventional statistical analysis (Sullivan and Feinn, 2012). A post hoc power analysis was not used to determine the sample size needed to detect significant effects between networks of patients with refractory and non-refractory IGE as post hoc analysis is misrepresentative as it does not indicate true power (Zhang *et al.*, 2019).

Nodal Volume analysis

FreeSurfer segmented volumes were used to compare each of the 82 network nodes for volume differences between subject groups using Cohen's d effect size calculation with small sample size correction (n<50) where $\bar{x}$ is the mean node volume of group 1 and $\bar{y}$ is the mean node volume of group 2 (see formula in Figure 1.C). An effect size analysis was used over statistical testing to determine the magnitude of difference between volume means for further downstream analysis. Based on Cohen (Cohen, 1992), d= 0.2 - 0.5 were considered small effect sizes, d = 0.5 - 0.8 medium effect sizes, d = 0.8 - 1.2 large effect sizes, and d > 1.2 very large effect sizes. All volumes were corrected for age, sex and ICV.

Network vs Nodal Volumes

To determine if NBS derived network alterations and nodal volume changes are linked, network based volume effects are computed (Figure 1.D). The 82 network nodes were split into nodes part of a significant NBS altered network (Figure 1.B) (NBS +) and unpertubed nodes (NBS -). Previously calculated volume differences (effect sizes) for the NBS (+) and NBS (–) nodes are compared using a Cohen's d calculation and significance (P<0.05) was determined using permutation testing (10,000 permutations). The resulting p-values were corrected for multiple comparisons using FDR correction; significance was set at $p<0.05_{FDR}$.

Results

NBS: diffusion-networks

Compared to controls, all patient groups had networks with significantly decreased Count and FA, and increased MD and RD metrics across a range of T-scores (p<0.05, |T| = 1.5 - 4.0). No AD alterations were found. The extent of network alterations differed in the patient groups relative to controls, with non-refractory patients having the fewest alterations across

FA, MD, and RD networks (Table 3, |T|>2.7). Analysis of FA networks revealed the most extensive network alterations across both cerebral hemispheres in the all patient group, and refractory IGE group relative to controls (Figure 2), with 54 significant edge alterations for all patients and 38 for patients with refractory IGE (Table 3, |T|>2.7). The most significant edges for each patient group for the FA networks were found bilaterally in the limbic and temporal lobes. Count, MD, and RD network differences are presented in the supplementary materials (Figure S1-3). There were no statistically significant network alterations found between patients with refractory and non-refractory IGE, although large and very large effect size differences were found between the treatment outcome groups (Figure S4).

Nodal volume analysis

The direction and magnitude of nodal volume differences (effect size) was dependent on group comparison and individual node (Figure 3). Patients with refractory IGE had decreased volumes whereas patients with non-refractory IGE had increased volumes compared to controls. Larger effect sizes were found for nodes in patients with non-refractory IGE relative to refractory IGE and controls. Volumetric differences between patients with IGE and controls were difficult to capture, compared to more robust differences found when separating out IGE patients into refractory and non-refractory groups.

Network vs Nodal Volumes

There were no statistically significant differences in the volume changes of NBS (+) and NBS (-) nodes for FA (Figure 4), Count (Figure S5), MD (Figure S6) or RD (Figure S7) structural networks for subject groups relative to controls, suggesting that the alterations in diffusion-based networks were not driven by nodal volume.

Discussion

In the present study we sought to determine diffusion-based structural network alterations in patients with refractory and non-refractory IGE using NBS. We report that patients with IGE show evidence of bihemispheric structural network alterations and that altered networks are manifest across a range of DTI metrics. The extent of network alterations depended on the network metric used; FA networks were predominantly affected. Patients who were non-refractory had reduced diffusion network alterations. We additionally sought to determine whether morphometric alterations in grey matter nodes were related to diffusion network alterations. We found no evidence to support this; nevertheless, patients with refractory IGE showed evidence of reduced grey matter volume, and patients with non-refractory IGE increased grey matter volume, relative to healthy controls.

Our results suggest widespread changes in white matter organisation in patients with IGE. We considered multiple diffusion metrics for network connection weights (edges) given that different metrics characterise various aspects of microscopic tissue alterations. Our network analysis is consistent with previous DTI tractography studies that have reported decreased FA and increased MD (Yang *et al.*, 2012; Focke *et al.*, 2014; Liang *et al.*, 2016; Qiu *et al.*, 2016; Knake *et al.*, 2017; Lobato *et al.*, 2018), increased RD (Focke *et al.*, 2014; Qiu *et al.*, 2016; Knake *et al.*, 2017) and no differences in AD (Knake *et al.*, 2017) in patients with IGE relative to controls. Decreased FA and increased MD suggests decreased isotropic diffusion which may be driven by a number of pathological processes affecting white matter tracts, such as demyelination (Alexander *et al.*, 2007; Winklewski *et al.*, 2018), a reduction in axonal density (Alexander *et al.*, 2007; Concha *et al.*, 2010; Garbelli *et al.*, 2012), or an increase in inflammation (Alexander *et al.*, 2007; Najjar *et al.*, 2011). Demyelination can also cause increased RD with minimal influence on AD (Winklewski *et al.*, 2018), which is equivalent to the pattern of findings we report. A literature review of 42 epilepsy and myelin studies (21 histological and 21 in vivo imaging) reported an association between epilepsy

and reduced myelin content (Drenthen *et al.*, 2020). However, these studies concentrate on focal epilepsies which has a different pathophysiology than IGE and therefore the underlying histopathology may be different. A histological human study of the healthy brain has found significant correlations between histological features of myelin and DTI metrics (Concha *et al.*, 2010; Seehaus *et al.*, 2015) which may suggest that our results could reflect altered myelin in IGE. However, as of yet, the exact underlying neurobiological alterations that drive DTI derived changes are not well understood in IGE.

Despite the existence of DTI studies of IGE, few have examined structural connectivity on an edge-by-edge global network perspective. NBS has previously been used to analyse structural connectivity in IGE (Caeyenberghs *et al.*, 2015). The authors reported a significantly increased streamline count in patients compared to controls. On the contrary, we report a decreased streamline count in similar regions (bilateral parietal and subcortical) in all patients relative to controls. Additionally, we found further streamline count changes in the cingulate and frontal regions. A combination of methodological discrepancies could potentially account for the differences, including composite of patient groups (refractory, non-refractory; IGE sybsyndromes) and inclusion of ICV (Smith *et al.*, 2020). Streamline count should be used with caution due to the nature of deterministic tracking algorithms (Jones and Cercignani, 2010) and it is easy to overinterpret results as tracking models contain many assumptions (Calamante, 2019). To reduce the likelihood of overinterpretation, we chose to assess multiple DTI metrics.

Previous DTI research has failed to show a clear biomarker of IGE drug resistance (Szaflarski *et al.*, 2016; Jiang *et al.*, 2017; Lobato *et al.*, 2018). Uncovering biomarkers of treatment outcome is important to provide better therapeutic management of patients (Gleichgerrcht and Bonilha, 2017), preventing seizures and reducing the morbidity of ineffective ASM side effects. To our knowledge we are the first to compare whole-brain structural networks between patients with refractory and non-refractory IGE, mirroring similar studies in TLE which show preoperative network analysis is predictive of postsurgical

outcomes using various network features (Bonilha *et al.*, 2013, 2015; Hutchings *et al.*, 2015; Munsell *et al.*, 2015; Gleichgerrcht *et al.*, 2018; Taylor *et al.*, 2018). Our results suggest network architecture differs between patients with refractory and non-refractory IGE relative to controls given that patients with non-refractory IGE had fewer network alterations than patients with refractory IGE and had increased nodal volumes. Grey matter volume increases have commonly been found in IGE (Woermann *et al.*, 1999; Betting *et al.*, 2006; Kim *et al.*, 2007; Bin *et al.*, 2017). Additionally, studies have found similar results of increased grey matter volumes specific to patients with non-refractory TLE relative to controls (Yasuda *et al.*, 2010; Doucet *et al.*, 2015). Volumetric node differences were more robust, and the directionality of volume results were in
oppositive directions when separating patients into groups based on their response to ASM, highlighting the distinct network architecture unique to each patient outcome group. Both network alterations and nodal volume alterations individually differ and do not appear to be related given that there was no significant difference between volumes of NBS (+) and NBS (-) nodes for all diffusion networks. This suggests a multifaceted difference in network architecture of refractory and non-refractory patients which may potentially make one network phenotype inherently less responsive to ASM. These complex network changes may potentially suggest a more advanced disease state in refractory epilepsy as described by the intrinsic disease severity hypothesis (Rogawski and Johnson, 2008). Alternatively, the increases in nodal grey matter volume found may be an indication of axonal sprouting and neuronal growth (Taupin, 2006; Tzarouchi *et al.*, 2009), both neuroplastic factors which occur during brain reorganisation (Stroemer, Kent and Hulsebosch, 1995; Carmichael, 2003; Bütefisch, 2006). This suggests the possibility that network architecture differences are less complex in patients with non-refractory IGE and they are potentially achieving seizure freedom through a form of neuroplasticity, a theory suggested previously in patients with TLE (Doucet *et al.*, 2015). However, other studies have suggested that increased grey matter in IGE may be due to other neuropathological factors such as microdysgenesis

(Woermann *et al.*, 1999). Overall, there is a necessity for further research into the pathophysiological mechanisms underpinning seizure freedom.

Limitations

There are some limitations to our study. Our cohort of patients with IGE were composed of different subsyndromes which may have different ictogenic mechanisms. However, these syndromes have many similarities, including clinical features (Reutens and Berkovic, 1995), underlying pathophysiological mechanisms including altered functional thalamic connectivity (Benuzzi *et al.*, 2012; Masterton, Carney and Jackson, 2012; Kim, Kim and Suh, 2019) and common genetic influences (De Kovel *et al.*, 2010). Therefore, similar network features may be found in mixed population subsyndromes and understanding these shared similarities is important. Furthermore, the refractory group were defined as having had seizures in the 12 months prior to recruitment and despite being homogenous in terms of being pharmacoresistant, it is possible multifactorial molecular and other biological mechanisms underlie refractoriness that may be different between patients (Tang et al.,2017). In cohort clinical studies such as ours, dichotomous groupings of refractory and non-refractory patients are frequently studied and may be helpful in identifying signatures of refractoriness using biological (Pollard et al., 2013; Wang et al., 2015), genetic (Gallek et al., 2016; Sun et al., 2016) and neuroimaging (Labate et al., 2015; Reddy et al., 2019) approaches.
One limitation of the study is the inconsistency of ASM regimes between patients, however, studies have found refractoriness in IGE does not depend on the type of ASM treatment (Marson *et al.*, 2007a, 2007b). Also, network alterations may precede the onset of IGE as suggested by studies of newly diagnosed epilepsy (Lee and Park, 2019; Kreilkamp *et al.*, 2021), or be a consequence of brain degeneration and/or remodelling in response to continued seizures. Longitudinal studies of newly diagnosed epilepsy are needed to determine if network alterations are a cause or effect of the disorder. Lastly, due to the small

sample size and uneven subgroups used in our study, no significant group differences between patients with refractory and non-refractory IGE were found using NBS. However, a Cohen's d effect size analysis for each edge in the diffusion networks between these subgroups showed small, medium, large and very large effect sizes depending on the edge (Figure S4). Future studies including a larger sample size of these subgroups may show edge differences to be significant.

Conclusions

Patients with IGE have widespread bihemispheric network alterations that differ between patients with refractory and non-refractory IGE relative to controls. The analysis of FA networks and nodal volumes yield the greatest differences between patient groups and provide evidence network alterations are multi-level (node and edge). Future work should prospectively examine the use of FA networks and node volumes as predictors of treatment outcome in newly diagnosed IGE.

Credit Author Statement

Andrea McKavanagh: Conceptualization, Methodology, Data curation, Software, Original draft preparation, Writing, Reviewing and Editing, Validation

Barbara A.K. Kreilkamp: Conceptualization, Methodology, Data curation, Software, Writing, Reviewing and Editing

Yachin Chen; Conceptualization, Methodology, Data curation

Christine Denby; Conceptualization, Data curation, Methodology

Martyn Bracewell; Conceptualization, Data curation, Methodology

Kumar Das: Conceptualization, Data curation, Methodology

Christophe De Dezenac: Data curation, Methodology

Anthony G. Marson: Conceptualization, Data curation, Methodology

Peter N. Taylor: Conceptualization, Methodology, Software, Writing, Reviewing and Editing, Supervision

Simon S. Keller: Conceptualization, Methodology, Writing, Reviewing and Editing, Validation, Supervision

Conflict of Interest Statement

None of the authors have any conflict of interest to disclose.

Funding and Acknowledgments

This work was supported by a UK Medical Research Council DiMeN DTP studentship awarded to AM and an ERUK project grant (Grant number 1085) awarded to SSK and PNT. SSK acknowledges support from the UK Medical Research Council (Grant Numbers MR/S00355X/1 and MR/K023152/1). PNT acknowledges support from the Wellcome Trust (105617/Z/14/ Z and 210109/Z/18/Z).

References

Alexander, A. L. *et al.* (2007) 'Diffusion Tensor Imaging of the Brain', *Neurotherapeutics*. doi: 10.1016/j.nurt.2007.05.011.

Baykan, B. *et al.* (2008) 'Myoclonic seizures subside in the fourth decade in juvenile myoclonic epilepsy.', *Neurology*. doi: 10.1212/01.wnl.0000313148.34629.1d.

Benuzzi, F. *et al.* (2012) 'Increased cortical BOLD signal anticipates generalized spike and wave discharges in adolescents and adults with idiopathic generalized epilepsies', *Epilepsia*. doi: 10.1111/j.1528-1167.2011.03385.x.

Berg, A. T. *et al.* (2010) 'Revised terminology and concepts for organization of seizures and epilepsies: Report of the ILAE Commission on Classification and Terminology, 2005-2009', *Epilepsia*, 51(4), pp. 676–685. doi: 10.1111/j.1528-1167.2010.02522.x.

Bernhardt, B. C. *et al.* (2009) 'Thalamo-cortical network pathology in idiopathic generalized epilepsy: Insights from MRI-based morphometric correlation analysis', *NeuroImage*. doi: 10.1016/j.neuroimage.2009.01.055.

Bernhardt, B. C., Bonilha, L. and Gross, D. W. (2015) 'Network analysis for a network disorder: The emerging role of graph theory in the study of epilepsy', *Epilepsy & Behavior*. Academic Press, 50, pp. 162–170. doi: 10.1016/J.YEBEH.2015.06.005.

Besson, P. *et al.* (2014) 'Structural connectivity differences in left and right temporal lobe epilepsy', *NeuroImage*. doi: 10.1016/j.neuroimage.2014.04.071.

Betting, L. E. *et al.* (2006) 'Voxel-based morphometry in patients with idiopathic generalized epilepsies', *NeuroImage*. doi: 10.1016/j.neuroimage.2006.04.174.

Bin, G. *et al.* (2017) ‘Patterns of gray matter abnormalities in idiopathic generalized epilepsy: A Meta-analysis of voxel-based morphology studies’, *PLoS ONE*. doi: 10.1371/journal.pone.0169076.

Bonilha, L. *et al.* (2013) *Presurgical connectome and postsurgical seizure control in temporal lobe epilepsy*, *Neurology*. doi: 10.1212/01.wnl.0000435306.95271.5f.

Bonilha, L. *et al.* (2015) ‘The brain connectome as a personalized biomarker of seizure outcomes after temporal lobectomy’, *Neurology*, 84(18), pp. 1846–1853. doi: 10.1212/WNL.0000000000001548.

Buchanan, C. R. *et al.* (2019) ‘The effect of network thresholding and weighting on structural brain networks in the UK Biobank’, *bioRxiv*. Elsevier Inc., p. 649418. doi: 10.1101/649418.

Bütefisch, C. M. (2006) ‘Neurobiological bases of rehabilitation’, *Neurological Sciences*. doi: 10.1007/s10072-006-0540-z.

Caeyenberghs, K. *et al.* (2015) ‘Hyperconnectivity in juvenile myoclonic epilepsy: A network analysis’, *NeuroImage: Clinical*. doi: 10.1016/j.nicl.2014.11.018.

Calamante, F. (2019) ‘The seven deadly sins of measuring brain structural connectivity using diffusion MRI streamlines fibre-tracking’, *Diagnostics*. doi: 10.3390/diagnostics9030115.

Carmichael, S. T. (2003) ‘Plasticity of cortical projections after stroke’, *Neuroscientist*. doi: 10.1177/1073858402239592.

Cockerell, O. C. *et al.* (1995) ‘Remission of epilepsy: results from the National General Practice Study of Epilepsy’, *The Lancet*. doi: 10.1016/S0140-6736(95)91208-8.

Cohen, J. (1992) ‘Quantitative Methods in Psychology: A Power Primer’, *Psychological Bulletin*.

Concha, L. *et al.* (2010) ‘In Vivo Diffusion Tensor Imaging and Histopathology of the Fimbria-Fornix in Temporal Lobe Epilepsy’, *Journal of Neuroscience*, 30(3), pp. 996–1002. doi: 10.1523/JNEUROSCI.1619-09.2010.

Desikan, R. S. *et al.* (2006) ‘An automated labeling system for subdividing the human cerebral cortex on MRI scans into gyral based regions of interest’, *NeuroImage*. doi: 10.1016/j.neuroimage.2006.01.021.

van Diessen, E. *et al.* (2013) ‘Functional and structural brain networks in epilepsy: What have we learned?’, *Epilepsia*. John Wiley & Sons, Ltd (10.1111), 54(11), pp. 1855–1865. doi: 10.1111/epi.12350.

Doucet, G. E. *et al.* (2015) ‘Frontal gray matter abnormalities predict seizure outcome in refractory temporal lobe epilepsy patients’, *NeuroImage: Clinical*. doi: 10.1016/j.nicl.2015.09.006.

Drenthen, G. S. *et al.* (2020) ‘On the merits of non-invasive myelin imaging in epilepsy, a literature review’, *Journal of Neuroscience Methods*. Elsevier, 338(January), p. 108687. doi: 10.1016/j.jneumeth.2020.108687.

Durlak, J. A. (2009) ‘How to select, calculate, and interpret effect sizes’, *Journal of Pediatric Psychology*. doi: 10.1093/jpepsy/jsp004.

Fisher, R. S. *et al.* (2017) ‘Operational classification of seizure types by the International League Against Epilepsy: Position Paper of the ILAE Commission for Classification and Terminology’, *Epilepsia*. doi: 10.1111/epi.13670.

Focke, N. K. *et al.* (2014) ‘Idiopathic-generalized epilepsy shows profound white matter diffusion-tensor imaging alterations’, *Human Brain Mapping*. doi:

10.1002/hbm.22405.

Gallek, M. J. *et al.* (2016) ‘Cortical gene expression: prognostic value for seizure outcome following temporal lobectomy and amygdalohippocampectomy’, *Neurogenetics*. doi: 10.1007/s10048-016-0484-2.

Garbelli, R. *et al.* (2012) ‘Blurring in patients with temporal lobe epilepsy: Clinical, high-field imaging and ultrastructural study’, *Brain*. doi: 10.1093/brain/aws149.

Gleichgerrcht, E. *et al.* (2018) ‘Deep learning applied to whole-brain connectome to determine seizure control after epilepsy surgery’, *Epilepsia*, 59(9), pp. 1643–1654. doi: 10.1111/epi.14528.

Gleichgerrcht, E. and Bonilha, L. (2017) ‘Structural brain network architecture and personalized medicine in epilepsy’, *Expert Review of Precision Medicine and Drug Development*. doi: 10.1080/23808993.2017.1364133.

Hutchings, F. *et al.* (2015) ‘Predicting Surgery Targets in Temporal Lobe Epilepsy through Structural Connectome Based Simulations’, *Plos Computational Biology*. 2015/12/15, 11(12), p. e1004642. doi: 10.1371/journal.pcbi.1004642.

Jallon, P. and Latour, P. (2005) ‘Epidemiology of idiopathic generalized epilepsies’, *Epilepsia*. doi: 10.1111/j.1528-1167.2005.00309.x.

Jiang, Y. *et al.* (2017) ‘Investigation of altered microstructure in patients with drug refractory epilepsy using diffusion tensor imaging’, *Neuroradiology*. doi: 10.1007/s00234-017-1835-x.

Jones, D. K. and Cercignani, M. (2010) ‘Twenty-five pitfalls in the analysis of diffusion MRI data’, *NMR in Biomedicine*, 23(7), pp. 803–820. doi: 10.1002/nbm.1543.

Kim, J. H. *et al.* (2007) ‘Regional grey matter abnormalities in juvenile myoclonic epilepsy: A voxel-based morphometry study’, *NeuroImage*. doi: 10.1016/j.neuroimage.2007.06.025.

Kim, J. H., Kim, J. Bin and Suh, S. il (2019) ‘Alteration of cerebello-thalamocortical spontaneous low-frequency oscillations in juvenile myoclonic epilepsy’, *Acta Neurologica Scandinavica*. doi: 10.1111/ane.13138.

Knake, S. *et al.* (2017) ‘Microstructural white matter changes and their relation to neuropsychological deficits in patients with juvenile myoclonic epilepsy’, *Epilepsy and Behavior*. Elsevier Inc., 76, pp. 56–62. doi: 10.1016/j.yebeh.2017.08.031.

De Kovel, C. G. F. *et al.* (2010) ‘Recurrent microdeletions at 15q11.2 and 16p13.11 predispose to idiopathic generalized epilepsies’, *Brain*. doi: 10.1093/brain/awp262.

Kramer, M. A. and Cash, S. S. (2012) ‘Epilepsy as a disorder of cortical network organization’, *Neuroscientist*, 18(4), pp. 360–372. doi: 10.1177/1073858411422754.

Kreilkamp, B. A. K. *et al.* (2021) ‘Altered structural connectome in non-lesional newly diagnosed focal epilepsy: Relation to pharmacoresistance’, *NeuroImage: Clinical*. doi: 10.1016/j.nicl.2021.102564.

Kwan, P. *et al.* (2010) ‘Definition of drug resistant epilepsy: Consensus proposal by the ad hoc Task Force of the ILAE Commission on Therapeutic Strategies’, *Epilepsia*, 51(6), pp. 1069–1077. doi: 10.1111/j.1528-1167.2009.02397.x.

Labate, A. *et al.* (2015) ‘White matter abnormalities differentiate severe from benign temporal lobe epilepsy’, *Epilepsia*. doi: 10.1111/epi.13027.

Lee, H. J. and Park, K. M. (2019) ‘Structural and functional connectivity in newly diagnosed juvenile myoclonic epilepsy’, *Acta Neurologica Scandinavica*. doi: 10.1111/ane.13079.

Liang, J. S. *et al.* (2016) 'Microstructural Changes in Absence Seizure Children: A Diffusion Tensor Magnetic Resonance Imaging Study', *Pediatrics and Neonatology*. doi: 10.1016/j.pedneo.2015.10.003.

Liao, W. *et al.* (2013) 'Relationship Between Large-Scale Functional and Structural Covariance Networks in Idiopathic Generalized Epilepsy', *Brain Connectivity*. doi: 10.1089/brain.2012.0132.

Liu, M. *et al.* (2011) 'Distinct white matter abnormalities in different idiopathic generalized epilepsy syndromes', *Epilepsia*. doi: 10.1111/j.1528-1167.2011.03313.x.

Lobato, M. *et al.* (2018) 'Analysis of fractional anisotropy and mean diffusivity in refractory and non-refractory idiopathic generalized epilepsies', *Seizure*. doi: 10.1016/j.seizure.2018.09.015.

Marson, A. G. *et al.* (2007a) 'The SANAD study of effectiveness of carbamazepine, gabapentin, lamotrigine, oxcarbazepine, or topiramate for treatment of partial epilepsy: an unblinded randomised controlled trial', *Lancet*. doi: 10.1016/S0140-6736(07)60460-7.

Marson, A. G. *et al.* (2007b) 'The SANAD study of effectiveness of valproate, lamotrigine, or topiramate for generalised and unclassifiable epilepsy: an unblinded randomised controlled trial', *Lancet*. doi: 10.1016/S0140-6736(07)60461-9.

Masterton, R. A., Carney, P. W. and Jackson, G. D. (2012) 'Cortical and thalamic resting-state functional connectivity is altered in childhood absence epilepsy', *Epilepsy Research*. doi: 10.1016/j.eplepsyres.2011.12.014.

Munsell, B. C. *et al.* (2015) 'Evaluation of machine learning algorithms for treatment outcome prediction in patients with epilepsy based on structural connectome data', *NeuroImage*, 118, pp. 219–230. doi: 10.1016/j.neuroimage.2015.06.008.

Najjar, S. *et al.* (2011) 'Refractory epilepsy associated with microglial activation', *Neurologist*. doi: 10.1097/NRL.0b013e31822aad04.

O'Muircheartaigh, J. *et al.* (2012) 'Abnormal thalamocortical structural and functional connectivity in juvenile myoclonic epilepsy', *Brain*. doi: 10.1093/brain/aws296.

Pollard, J. R. *et al.* (2013) 'TheTARC/sICAM5 ratio in patient plasma is a candidate biomarker for drug resistant epilepsy', *Frontiers in Neurology*. doi: 10.3389/fneur.2012.00181.

Qi, S. *et al.* (2015) 'The influence of construction methodology on structural brain network measures: A review', *Journal of Neuroscience Methods*. doi: 10.1016/j.jneumeth.2015.06.016.

Qiu, W. *et al.* (2016) 'Structural abnormalities in childhood absence epilepsy: Voxel-based analysis using diffusion tensor imaging', *Frontiers in Human Neuroscience*. doi: 10.3389/fnhum.2016.00483.

Qiu, W. *et al.* (2017) 'Disrupted topological organization of structural brain networks in childhood absence epilepsy', *Scientific Reports*. doi: 10.1038/s41598-017-10778-0.

Reddy, S. D. *et al.* (2019) 'Neuroimaging biomarkers of experimental epileptogenesis and refractory epilepsy', *International Journal of Molecular Sciences*. doi: 10.3390/ijms20010220.

Reutens, D. C. and Berkovic, S. F. (1995) 'Idiopathic generalized epilepsy of adolescence: Are the syndromes clinically distinct?', *Neurology*. doi: 10.1212/WNL.45.8.1469.

Rogawski, M. A. and Johnson, M. R. (2008) 'Intrinsic Severity as a Determinant of Antiepileptic Drug Refractoriness', *Epilepsy Currents*. doi: 10.1111/j.1535-

7511.2008.00272.x.

Sarwar, T. *et al.* (2019) ‘Mapping connectomes with diffusion MRI: deterministic or probabilistic tractography?’, *Magn Reson Med*, 81(2), pp. 1368–1384. doi: 10.1002/mrm.27471.

Scheffer, I. E. *et al.* (2017) ‘ILAE classification of the epilepsies: Position paper of the ILAE Commission for Classification and Terminology’, *Epilepsia*. doi: 10.1111/epi.13709.

Seehaus, A. *et al.* (2015) ‘Histological validation of high-resolution DTI in human post mortem tissue’, *Frontiers in Neuroanatomy*, 9(JULY), pp. 1–12. doi: 10.3389/fnana.2015.00098.

Semah, F. *et al.* (1998) ‘Is the underlying cause of epilepsy a major prognostic factor for recurrence?’, *Neurology*, 51(5), pp. 1256–1262. doi: 10.1212/WNL.53.2.437-e.

Seneviratne, U., Cook, M. and D’Souza, W. (2012) ‘The electroencephalogram of idiopathic generalized epilepsy’, *Epilepsia*. doi: 10.1111/j.1528-1167.2011.03344.x.

Smith, R. *et al.* (2020) ‘Quantitative streamlines tractography: methods and inter-subject normalisation’, (c), pp. 1–27. doi: 10.31219/osf.io/c67kn.

Smith, S. M. *et al.* (2004) ‘Advances in functional and structural MR image analysis and implementation as FSL’, *NeuroImage*, 23(SUPPL. 1), pp. 208–219. doi: 10.1016/j.neuroimage.2004.07.051.

Sone, D. *et al.* (2019) ‘Reduced resilience of brain gray matter networks in idiopathic generalized epilepsy: A graph-theoretical analysis’, *PLOS ONE*. Edited by B. C. Bernhardt. Public Library of Science, 14(2), p. e0212494. doi: 10.1371/journal.pone.0212494.

Spencer, S. S. (2002) ‘Neural Networks in Human Epilepsy : Evidence of and Implications for Treatment’, *Epilepsia*, 43(3), pp. 219–227. doi: 10.1046/j.1528-1157.2002.26901.x.

Stroemer, R. P., Kent, T. A. and Hulsebosch, C. E. (1995) ‘Neocortical neural sprouting, synaptogenesis, and behavioral recovery after neocortical infarction in rats’, *Stroke*. doi: 10.1161/01.STR.26.11.2135.

Sullivan, G. M. and Feinn, R. (2012) ‘ Using Effect Size—or Why the P Value Is Not Enough ’, *Journal of Graduate Medical Education*. doi: 10.4300/jgme-d-12-00156.1.

Sun, Y. *et al.* (2016) ‘Expression of microRNA-129-2-3p and microRNA-935 in plasma and brain tissue of human refractory epilepsy’, *Epilepsy Research*. doi: 10.1016/j.eplepsyres.2016.09.016.

Szaflarski, J. P. *et al.* (2016) ‘White matter abnormalities in patients with treatment-resistant genetic generalized epilepsies’, *Medical Science Monitor*. doi: 10.12659/MSM.897002.

Taupin, P. (2006) ‘Adult neurogenesis and neuroplasticity’, *Restorative Neurology and Neuroscience*.

Taylor, P. N. *et al.* (2015) ‘Structural connectivity changes in temporal lobe epilepsy: Spatial features contribute more than topological measures’, *NeuroImage: Clinical*. Elsevier B.V., 8, pp. 322–328. doi: 10.1016/j.nicl.2015.02.004.

Taylor, P. N. *et al.* (2018) ‘The impact of epilepsy surgery on the structural connectome and its relation to outcome’, *NeuroImage: Clinical*. Elsevier, 18, pp. 202–214. doi: 10.1016/j.nicl.2018.01.028.

Tzarouchi, L. C. *et al.* (2009) ‘Periventricular leukomalacia in preterm children: Assessment of grey and white matter and cerebrospinal fluid changes by MRI’,

Pediatric Radiology. doi: 10.1007/s00247-009-1389-0.

Vulliemoz, S. *et al.* (2011) 'Connectivity of the supplementary motor area in juvenile myoclonic epilepsy and frontal lobe epilepsy', *Epilepsia*. doi: 10.1111/j.1528-1167.2010.02770.x.

Wang, J. *et al.* (2015) 'Circulating microRNAs are promising novel biomarkers for drug-resistant epilepsy', *Scientific Reports*. doi: 10.1038/srep10201.

Wei, K. *et al.* (2017) 'Sensitivity analysis of human brain structural network construction'. doi: 10.1162/netn_a_00025.

Winklewski, P. J. *et al.* (2018) 'Understanding the physiopathology behind axial and radial diffusivity changes-what do we Know?', *Frontiers in Neurology*, 9(FEB). doi: 10.3389/fneur.2018.00092.

Woermann, F. G. *et al.* (1999) 'Abnormal cerebral structure in juvenile myoclonic epilepsy demonstrated with voxel-based analysis of MRI', *Brain*. doi: 10.1093/brain/122.11.2101.

Xue, K. *et al.* (2014) 'Diffusion tensor tractography reveals disrupted structural connectivity in childhood absence epilepsy', *Epilepsy Research*. doi: 10.1016/j.eplepsyres.2013.10.002.

Yang, T. *et al.* (2012) 'White matter impairment in the basal ganglia-thalamocortical circuit of drug-naïve childhood absence epilepsy', *Epilepsy Research*. doi: 10.1016/j.eplepsyres.2011.12.006.

Yasuda, C. L. *et al.* (2010) 'Dynamic changes in white and gray matter volume are associated with outcome of surgical treatment in temporal lobe epilepsy', *NeuroImage*. doi: 10.1016/j.neuroimage.2009.08.014.

Yeh, F. C. *et al.* (2013) 'Deterministic diffusion fiber tracking improved by quantitative anisotropy', *PLoS ONE*, 8(11), pp. 1–16. doi: 10.1371/journal.pone.0080713.

Yeh, F. C. *et al.* (2019) 'Automatic Removal of False Connections in Diffusion MRI Tractography Using Topology-Informed Pruning (TIP)', *Neurotherapeutics*. Neurotherapeutics, 16(1), pp. 52–58. doi: 10.1007/s13311-018-0663-y.

Yeh, F. C., Wedeen, V. J. and Tseng, W. Y. I. (2010) 'Generalized q-sampling imaging', *IEEE Transactions on Medical Imaging*, 29(9), pp. 1626–1635. doi: 10.1109/TMI.2010.2045126.

Zalesky, A., Fornito, A. and Bullmore, E. T. (2010) 'Network-based statistic: Identifying differences in brain networks', *NeuroImage*. Elsevier Inc., 53(4), pp. 1197–1207. doi: 10.1016/j.neuroimage.2010.06.041.

Zhang, Y. *et al.* (2019) 'Post hoc power analysis: Is it an informative and meaningful analysis?', *General Psychiatry*. doi: 10.1136/gpsych-2019-100069.

Zhang, Z. *et al.* (2011) 'Altered functional-structural coupling of large-scale brain networks in idiopathic generalized epilepsy', *Brain*. Oxford University Press, 134(10), pp. 2912–2928. doi: 10.1093/brain/awr223.

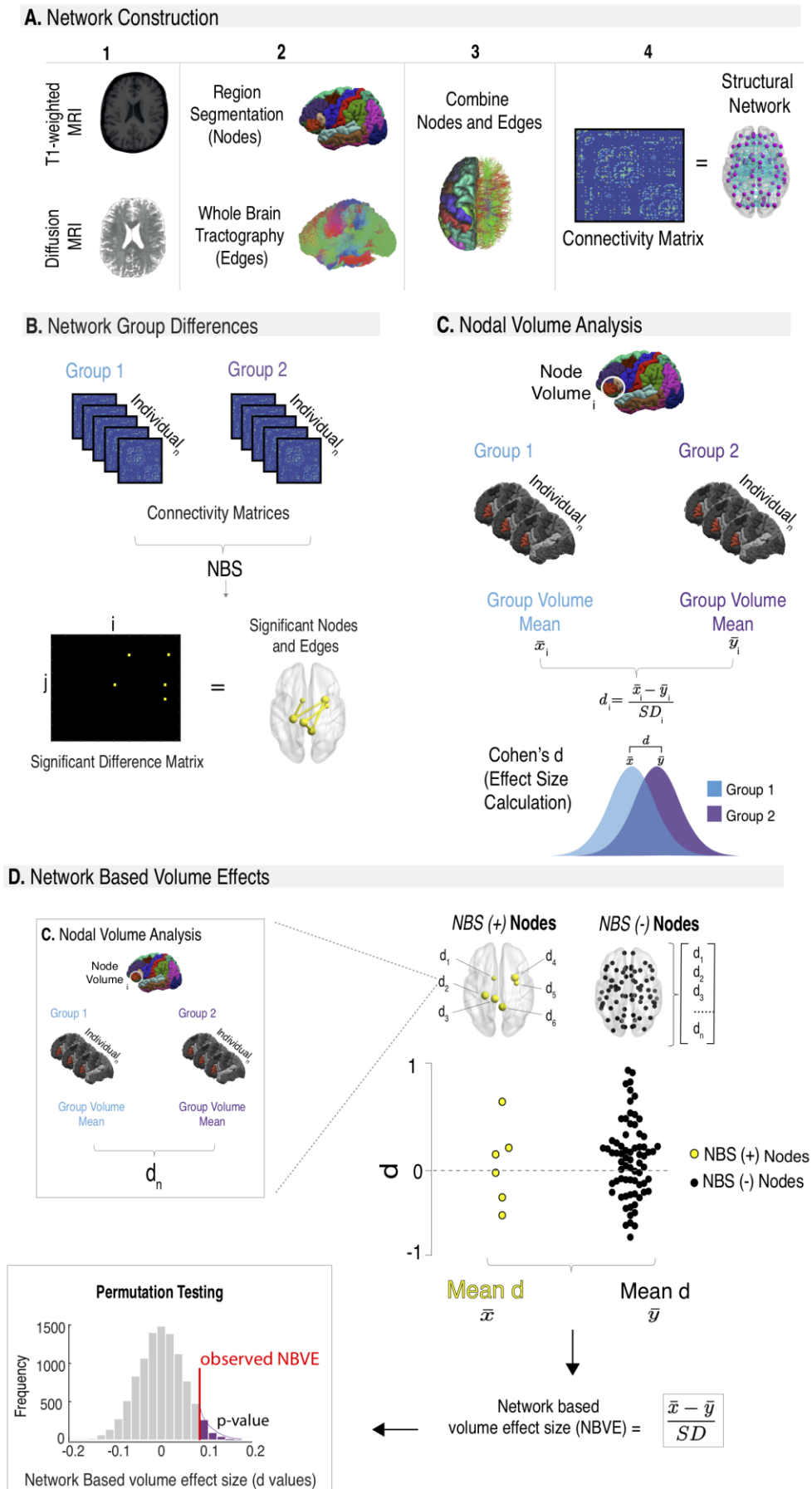
A. Network Construction
1
2
3
4
T1-weighted MRI
Diffusion MRI
Region Segmentation (Nodes)
Whole Brain Tractography (Edges)
Combine Nodes and Edges
Connectivity Matrix
Structural Network
B. Network Group Differences
Group 1
Group 2
Individual n
Connectivity Matrices
NBS
i
j
Significant Difference Matrix
Significant Nodes and Edges
C. Nodal Volume Analysis
Node Volume i
Group Volume Mean
Cohen's d (Effect Size Calculation)
Group 1
Group 2
D. Network Based Volume Effects
NBS (+) Nodes
NBS (-) Nodes
Mean d
Network based volume effect size (NBVE) =
Permutation Testing
Frequency
observed NBVE
p-value
Network Based volume effect size (d values)

Figure 1. Structural Network analysis method: (A) Network construction using T1w and diffusion weighted MRI scans. T1w scans are segmented into 82 regions (nodes) based on the FreeSurfer Desikan-Killiany atlas. Whole brain tractography of diffusion MRI scans is performed in DSI studio to give connection weights of streamline count (Count), fractional anisotropy (FA), mean diffusivity (MD), axial diffusivity (AD) and radial diffusivity (RD) between nodes representing network edges. Nodes and edges are combined to form Count, FA, MD, AD and RD structural networks which can be viewed in matrix (inputs representing connections) or network form. (B) Structural networks of subject group pairs (all patients vs controls; refractory vs controls; non-refractory vs controls; refractory vs non-refractory) are compared using Network Based Statistics (NBS). NBS outputs a difference matrix consisting of significant ($p<0.05$) node pairs (i and j) and edges (matrix inputs C_{ij}) which differ between groups and can be visualised as a structural network. (C) Volumes for each of the 82 network nodes (i) from the FreeSurfer segmentations are compared between subject group pairs using a Cohen's d effect size calculation. (D) Network-Based volume effects (NBVE) are calculated by comparing volume differences (effect sizes) of nodes from altered networks (NBS +) and unperturbed nodes (NBS -) using a Cohen's d calculation. Significance ($p<0.05$) is determined using permutation testing.

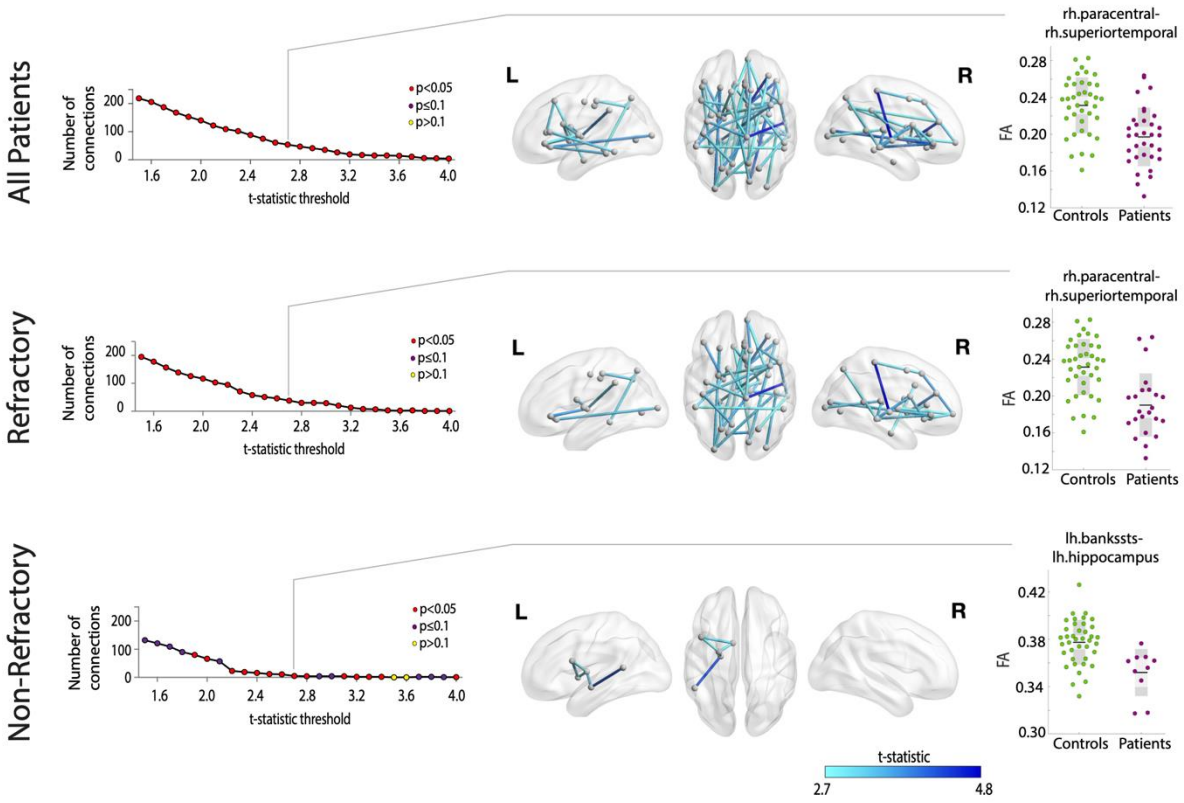

Figure 2. Significant network FA differences between subject groups relative to controls (decreased FA; p<0.05; threshold of T = 2.7). Graphs represent the number of significantly altered network edges over a range of NBS thresholds. The glass brains visually show the altered networks at T≥2.7 with edge colour representing the t-statistic. Boxplots of the most significant edge and corresponding node names is also found.

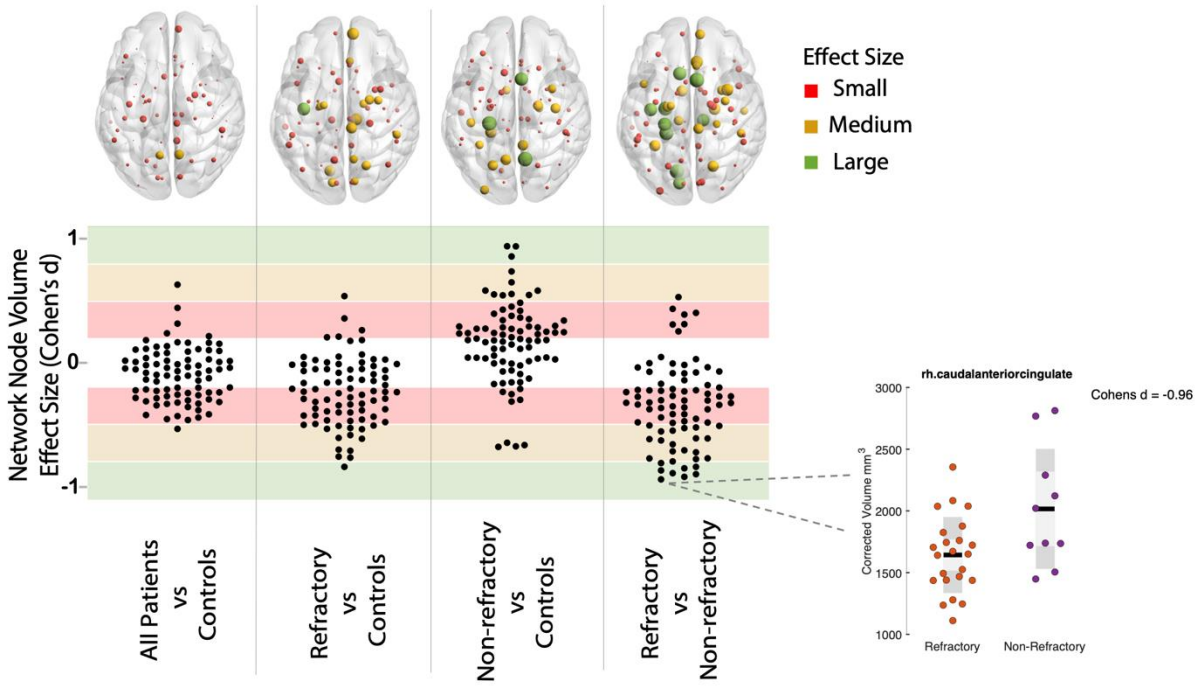

Figure 3. Network node grey matter volume differences between subject group pairs using Cohen's d effect size calculation. Box plots show Cohen's d values for individual nodes between subject group pairs. Legend colours represent the levels of effect size differences. Glass brains visually show nodal volume differences with nodal size corresponding to effect size and colour representing the effect size level.

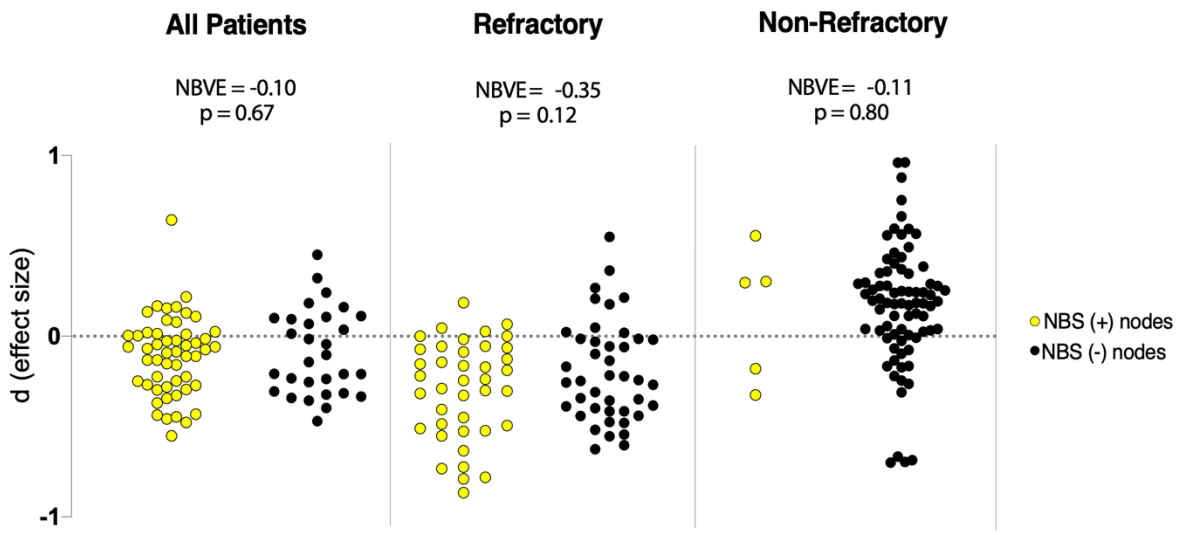

Figure 4. FA network-based volume effects (NBVE). Comparisons of the volume differences (effect sizes) between NBS (+) (nodes from significantly altered FA network) and NBS (-) nodes (unperturbed FA nodes) of subject groups relative to controls. Cohen's d calculation is applied to compute an NBVE value and significance ($p<0.05$) is determined using permutation testing (10,000 permutations).